Analytical, State-Space, Full Bridge MMC model

Dragan Jovcic, *Fellow IEEE, and* Jean Mahseredjian, *Fellow IEEE*

***Abstract*— This paper presents the development of a small signal analytical state-space model for a Full Bridge MMC converter. Building on the existing Half Bridge MMC analytical model, all new model equations are derived considering the new control variable, DC modulation index M_{dc}. The model is of 29th order, and it is developed in 3 rotating dq coordinate frames: zero sequence, fundamental frequency and second harmonic.**

The model is verified against detailed non-linear EMTP model for a 1 GW, 640 kV MMC test system. The verification demonstrates good accuracy for all model variables considering a range of inputs on the reference and disturbance signals.

The developed model is employed to study eigenvalues position as the M_{dc} controller gains change, and it is concluded that M_{dc} controller improves damping of the dominant oscillatory mode.

***Index Terms*—Full bridge MMC converter, HVDC transmission,**

I. Introduction

MMC (Modular Multilevel Converters) have become the predominant technology for HVDC (High Voltage Direct Current) transmission in the last 10 years [1]. Virtually all installed MMC HVDC employ HB (Half Bridge) converters. However, the German Ultranet HVDC project, (in the final construction phase in 2021), utilizes FB (Full Bridge) converters, that enable excellent DC fault handling with HVDC based on overhead lines. FB-based HVDC also brings other advantages like better operating flexibility and recovery [2][3], and they have advantages in switchgear costs when building DC transmission grids [4].

Simulation of MMC converters is commonly based on EMT-type platforms using non-linear models in time domain [5]. A range of EMTP MMC models is available giving user a tradeoff choice between level of detail and simulation time [6]. Nevertheless, EMTP simulation supports mainly time-domain trial-and-error studies, which are time consuming with complex multi-dimensional problems.

The analytical dynamic models have been used for power system studies for many years [1], and they have been developed for HB MMC converters recently [7][8]. When linearized, they provide LTI (Linear Time Invariant) format which is convenient for the application of all modern methods for dynamic analysis and control design. They enable qualitative studies and generic design approaches.

The 10th order linearized state-space MMC model in [8] considers only HB converter topology. Although operating principles of FB MMC are well understood, an analytical FB MMC model has not yet been reported.

Building on the model in [8], this paper aims developing FB MMC small-signal state-space LTI model. The basic controllers will also be included, considering normal *dq* current control on AC side, but also using DC modulation index control input, characteristic for FB MMC topology.

The goal is to present the key additional/modified equations necessary to expand HB model into FB topology, and to test and verify accuracy. The verification will be performed utilizing detailed non-linear simulation on EMTP.

II. Test Circuit and Model Structure

The test circuit consists of a single MMC converter connected to an equivalent AC system and a simple T-model for the DC cable, as shown in Fig. 1. The key parameters of the 1GW MMC test system are shown in Fig. 1, while detailed circuit structure can be found in the EMTP MMC models [6].

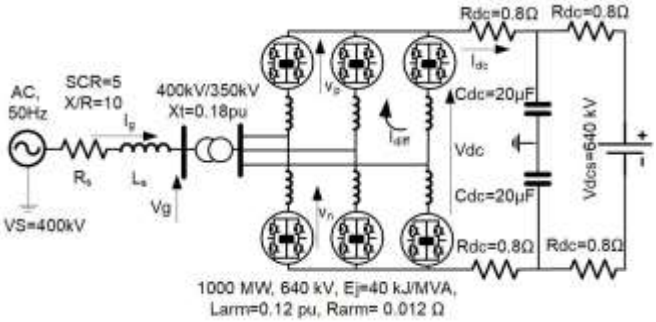

Fig. 1. Test circuit for verification FB MMC model.

III. MMC Converter Model

The method of deriving 10th order dynamic model of HB MMC is given in [1],[8], and all the variables and parameters adopt the notation given therein. All the modeling principles and majority of equations apply also to FB MMC. The primary difference with FB MMC is that the control signal has an additional variable M_{dc} that facilitates variation of the average value of the arm control signal. Utilizing the HB MMC control signal description [1], the ABC-frame expressions for control signals for positive arm m_P and negative arms m_N of a FB MMC can be derived:

$$m_P = \frac{1}{2}(M_{dc} - M_{ac}\,cos(\omega t + \theta_m)), \quad -1 < m_P < 1 \qquad (1)$$

$$m_N = \frac{1}{2}(M_{dc} + M_{ac}\,cos(\omega t + \theta_m)), \quad -1 < m_N < 1 \qquad (2)$$

where M_{ac} and θ_m are the two control signals with HB MMC (they become M_d and M_q in the *dq* rotating frame), and the expression converts to standard HB version when $M_{dc}=1$. The FB ability of negative cell voltage defines the range of control signals:

$$0 < M_{ac} < 1, \quad -1 < M_{dc} < 1 \qquad (3)$$

and enables wider range of arm control signals as in (1),(2). The two basic dynamic equations for MMC arms are [1]:

This project has received funding from the Royal Society exchange grant.
D. Jovcic is with the University of Aberdeen, AB24 3UE, U.K. (d.jovcic@abdn.ac.uk).

J Mahseredjian . is with Polytechnique Montreal, Canada, jean.mahseredjian@polymtl.ca)

$$v_P^M = \frac{m_P}{sC_{arm}}(i_{diff} + \frac{i_g}{2}) \quad (4)$$

$$v_N^M = \frac{m_N}{sC_{arm}}(i_{diff} - \frac{i_g}{2}) \quad (5)$$

where s is LaPlace operator, v_p^M and v_p^M are maximal arm voltages, i_{diff} is differential current, i_g is grid current, C_{arm} is the arm capacitance, and all parameters follow terminology from [8] and [1]. Replacing (1) and (2) in (4) and (5) the two corresponding non-linear dynamic equations are obtained with variables comprised of zero-sequence (*0*), fundamental (*dq*) and second harmonics (*d2q2*). The model is separated into 3 coordinate frames utilizing algebra for *dq* frame modeling [8]. Only the equations that contain new M_{dc} variable will be presented, while others are equal to the HB model.

In the zero-sequence coordinate frame, the dynamic equation for zero sequence of the maximal arm voltage becomes V_{P0}^M:

$$v_{P0}^M = \frac{1}{s2C_{arm}}\left(M_{dc}i_{diff0} + \frac{M_d i_{gd}}{2} + \frac{M_q i_{gq}}{2} + \frac{M_{d2} i_{diffd2}}{2} + \frac{M_{q2} i_{diffq2}}{2}\right) \quad (6)$$

In the *dq* coordinate frame the fundamental components of the maximal arm voltages will also depend on the M_{dc} variable:

$$v_{Pd}^M = \frac{1}{sC_{arm}}\left(\frac{M_q}{2} i_{diff0} - \frac{M_q}{4} i_{diffd2} + \frac{M_d}{4} i_{diffq2} - \frac{M_{dc}}{4} I_{gq}\right) \quad (7)$$

$$v_{Pq}^M = \frac{1}{sC_{arm}}\left(-\frac{M_d}{2} i_{diff0} - \frac{M_d}{4} i_{diffd2} - \frac{M_q}{4} i_{diffq2} + \frac{M_{dc}}{4} i_{gd}\right) \quad (8)$$

In the *d2q2* coordinate frame (rotating at 2ω) the dynamics of second harmonic of the maximal arm voltage become [1]:

$$v_{Nq2}^M = \frac{1}{s2C_{arm}}\left(\frac{M_{dc}}{2} i_{diffd2} - \frac{M_d i_{gd}}{8} + \frac{M_q i_{gq}}{8}\right) \quad (9)$$

$$v_{Nd2}^M = \frac{1}{s2C_{arm}}\left(-\frac{M_{dc}}{2} i_{diffq2} + \frac{M_q I_{gd}}{8} + \frac{M_d I_{gq}}{8}\right) \quad (10)$$

Also the following 2 (static) output equations depend on M_{dc}:

$$v_P = m_P v_P^M \quad (11)$$

$$v_N = m_N v_N^M \quad (12)$$

When expanded, (11) and (12) will give the arm AC voltages:

$$v_{Pd} = -\frac{1}{2}M_d v_{P0}^M + \frac{1}{2}M_{dc} v_{Pd}^M - \frac{1}{4}M_d v_{Pd2}^M - \frac{1}{4}M_q v_{Pq2}^M \quad (13)$$

$$v_{Pq} = -\frac{1}{2}M_q v_{P0}^M + \frac{1}{2}M_{dc} v_{Pq}^M + \frac{1}{4}M_q v_{Pd2}^M - \frac{1}{4}M_d v_{Pq2}^M \quad (14)$$

Further, zero sequence of (4) and (5) will give the following:

$$M_{dc} I_{diff0} = \frac{1}{4}M_d I_{gd} + \frac{1}{4}M_q I_{gq} \quad (15)$$

Assuming a symmetrical system $I_{dc}=3I_{diff0}$, then (15) gives:

$$I_{dc} = \frac{3}{4}\frac{M_d i_{gd} + M_q i_{gq}}{M_{dc}} \quad (16)$$

Equations (16) and (7) give the key link between control signal M_{dc} and the maximal arm voltage v_{pd0}^M. The above equations are linearized and incorporated in the state-space matrices of the linearized MMC model.

IV. Controller Model

There are various options to develop controller for FB MMC [3][4], and for the purpose of demonstrating model accuracy only a simple controller is used as shown in Fig. 2. The upper part with M_d and M_q signal is identical as with HB MMC [1], while the M_{dc} signal is added for FB MMC.

The M_{dc} control signal is employed to regulate the average zero-sequence maximal arm voltage, which is similar as arm energy control studied in [7]. The reference value for the maximal arm voltage is set slightly above the value for DC voltage V_{cp0}=*650 kV* (while V_{dcs}=*640 kV*).

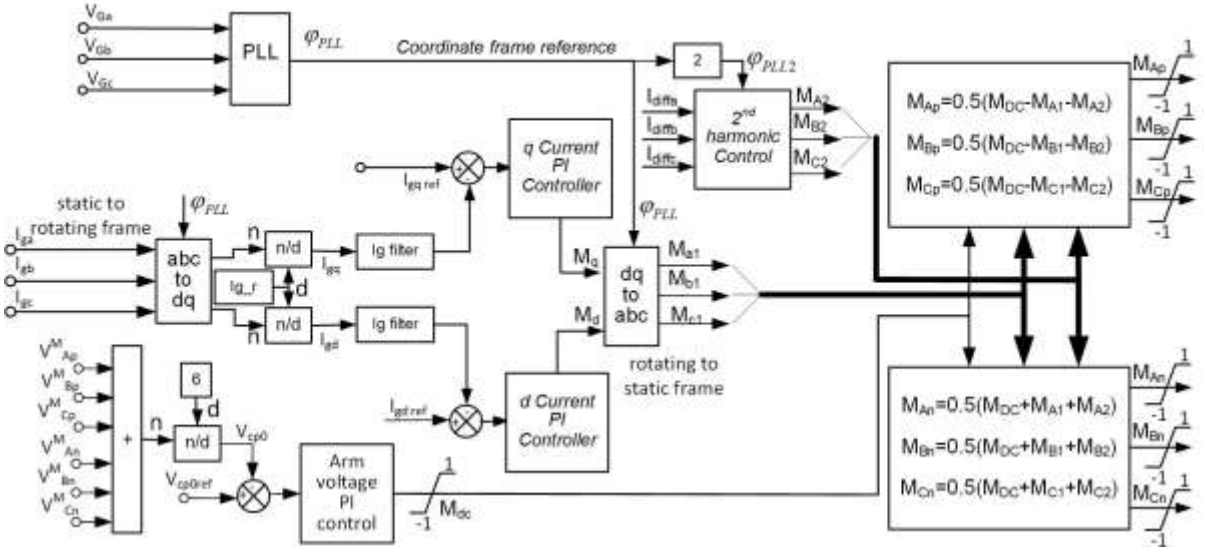

Fig. 2. A simple FB MMC controller.

This leads to nominal value for M_{dc} of around 0.97, which gives some room for control action in the upper direction. The PLL model assumes standard *dqz* structure [1],[9].

V. FB MMC STATE-SPACE MODEL

The final state space model is of 29^{th} order and consist of:

- AC system – 6^{th} order, which includes an artificial state to provide V_g accessible as a state variable,
- Phase locked loop – 2^{nd} order,
- MMC model – 14^{th} order. 10^{th} order includes circulating current control as in [8], with 2 second order filters for the second harmonic circulating current.
- Controller – 6^{th} order, consisting of 3 PI controls.
- DC system 1^{st} order.

All the model segments are connected into a single state-space model which is coded as an LTI model in MATLAB.

VI. MODEL VERIFICATION

The model is verified for various reference and disturbance inputs. Linearized state-space models are valid only for small variations around steady-state, and therefore *5%* signal magnitude is used. Large disturbances cannot be studied, but the model can be used to evaluate stability at a new operating point under a fault. All 29 model states are monitored to enable verification of accuracy of all subsystems and modes.

Fig. 3 shows the simulation of 32 kV DC source voltage V_{dcs} (disturbance signal) drop. It is seen that the M_{dc} controller reacts on this disturbance by reducing M_{dc} and preventing large DC current. Crucially, it maintains maximal arm voltage at the reference value. This is the key FB functionality that enables riding through DC faults, and maintaining AC-side controls. M_{dc} control therefore shields AC side of MMC from disturbances on the DC side. Observing (13) and (14) it is seen that the maximal arm voltage $V_{P0}{}^{M}$ should be maintained constant in order to enable good control of AC voltages.

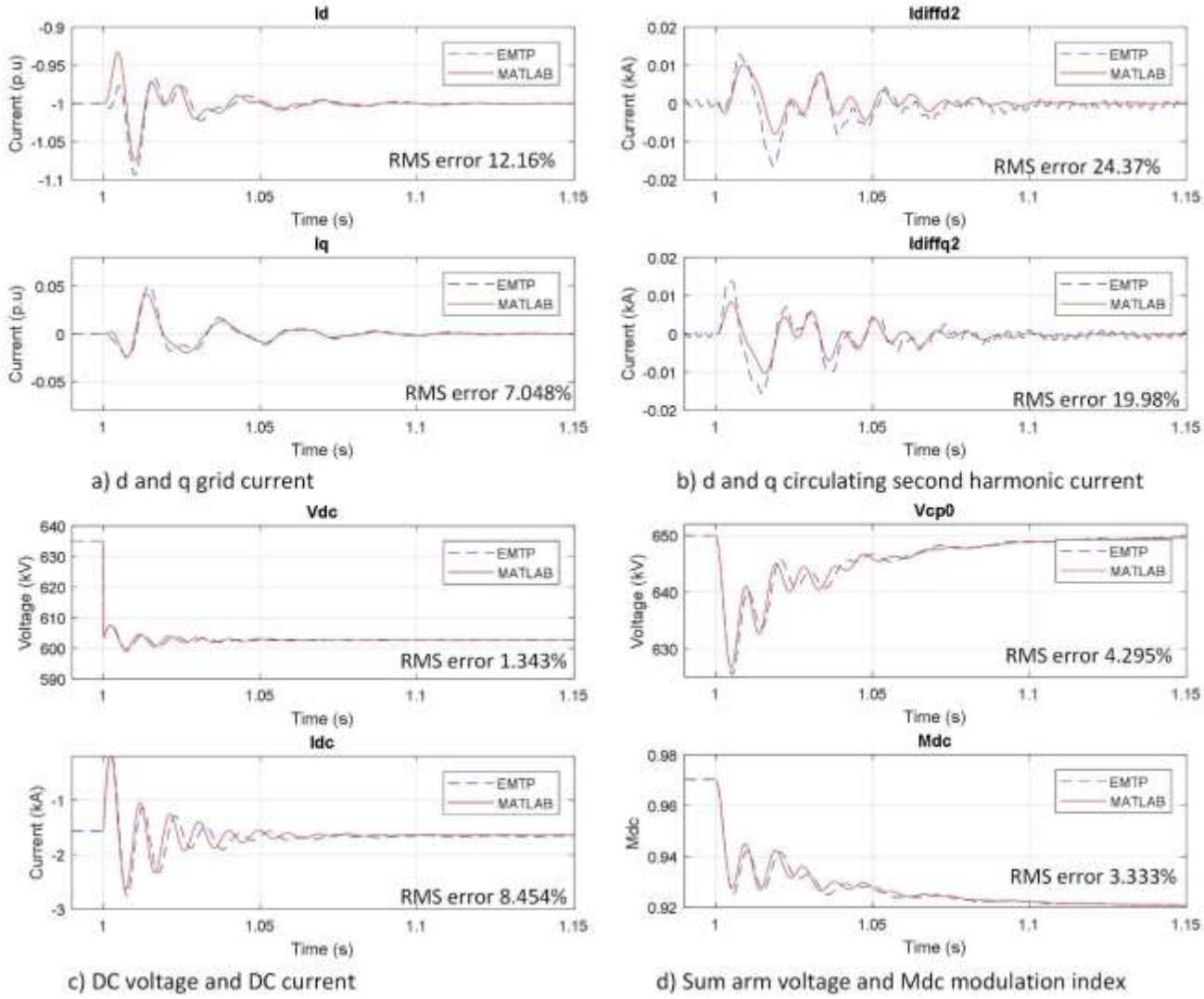

Fig. 3. Analytical and EMTP-RV model response for a 5% DC source voltage drop.

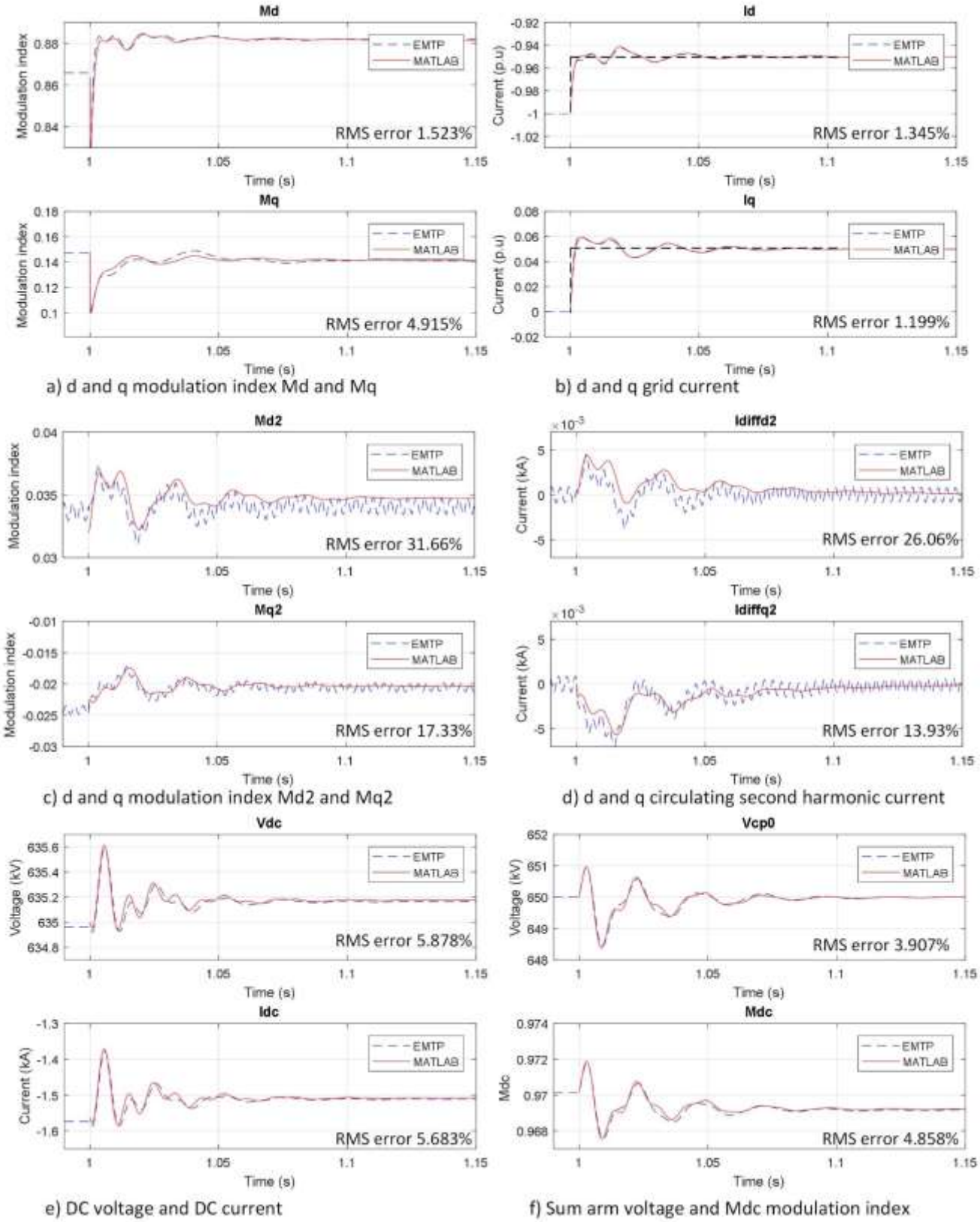

Fig. 4. Analytical and EMTP-RV model response for a 5% simultaneous step on I_{dref} and I_{qref}.

It is observed that different model segments have different oscillatory modes, and they are all quite well captured with the analytical model. It is also seen that all model variables show good matching with the detailed nonlinear EMTP model variables. The relative RMS error is calculated for each variable using difference between EMTP variable and MATLAB variable over the simulation period, and then scaled with the peak deviation of the particular variable. The differential currents (I_{diffd2} and I_{diffq2}) show large (over 20%) RMS error, caused mainly by the steady-state 6^{th} harmonic (300Hz) on *d2q2* variables. MATLAB model cannot represent 3^{rd} harmonic which is present in steady-state, and shows as 6^{th} harmonic in the second harmonic (*d2q2*) coordinate frame. The solution would be introduce additional 3^{rd} harmonic coordinate frame (*d3q3*) as it is done with HB MMC model in [7]. The other mismatch with MATLAB variables is the result of unmodelled parasitics and also linearization.

Fig. 4 shows verification of wider range of model variables for two simultaneous reference steps (*-5%* on I_{dref} and *+5%* on I_{qref}). It is seen that different oscillatory modes are excited compared with the V_{dc} reference step in Fig. 3. It is concluded that the analytical model shows good accuracy for all variables and all dominant dynamics.

VII. Example eigenvalue study

Fig. 5 shows the eigenvalue position as the M_{dc} PI controller gain is increasing from zero to twice the selected value for the test system, keeping controller zero constant (*ki/kp=40*). The initial value, given by the blue circles, corresponds to the HB system (no M_{dc} control). The selected value is shown by green diamonds. It is seen that the damping of the dominant oscillatory mode at around *35 Hz* is improving but the other two oscillatory modes at around *90-100 Hz* experience small deterioration in damping with M_{dc} control.

It is underlined that this type of analysis on such complex system would be very challenging with EMTP simulation.

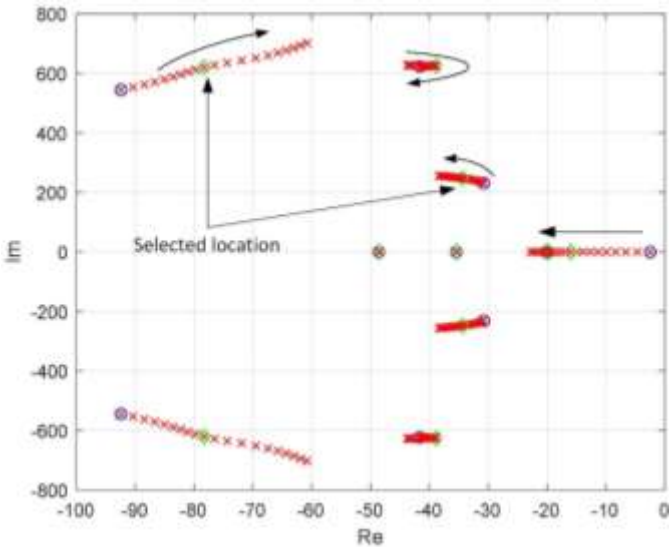

Fig. 5. Eigenvalue position as the FB controller gains increase.

VIII. Conclusions

The paper presents a small signal analytical state-space model for a Full Bridge MMC converter. It is shown that one new variable, DC modulation index M_{dc}, should be introduced in order to expand the existing HB MMC analytical model. This variable however impacts many of the equations in all 3 coordinate frames of the MMC model, and therefore the dynamics will be significantly affected.

The model verification against detailed non-linear EMTP model demonstrates good accuracy for all model variables, and for different excitation inputs.

The developed model is used to study eigenvalues position as the M_{dc} controller gains change, and it is concluded that M_{dc} controller improves damping of the dominant oscillatory mode.

References

[1] D Jovcic "High-Voltage Direct Current Transmission: Converters Systems and DC Grids", second edition, Wiley 2019.

[2] Zeng R, Xu L, Yao L, Williams B. Design and operation of a hybrid modular multilevel converter. *IEEE Transactions on Power Electronics* 2015; 30: 1137-1146.

[3] M. Stumpe, P. Ruffing, P. Wagner and A. Schnettler, "Adaptive Single-Pole Autoreclosing Concept with Advanced DC Fault Current Control for Full-Bridge MMC VSC Systems," in *IEEE Transactions on Power Delivery*, vol. 33, no. 1, pp. 321-329, Feb. 2018,

[4] D. Jovcic, W. Lin, S. Nguefeu and H. Saad, "Low-Energy Protection System for DC Grids Based on Full-Bridge MMC Converters," in *IEEE Transactions on Power Delivery*, vol. 33, no. 4, pp. 1934-1943, Aug. 2018.

[5] J. Mahseredjian, S. Dennetière, L. Dubé, L., B.Khodabakhchian, L. Gérin-Lajoiee, "On a New Approach for the Simulation of Transients in Power Systems," *Electric Power Systems Research*, vol. 77, no. 1, pp. 1514-1520, Sep. 2007

[6] H. Saad, S. Dennetière, J. Mahseredjian, P. Delarue, X. Guillaud, J. Peralta, et al., "Modular multilevel converter models for electromagnetic transients," IEEE Transactions on Power Delivery, vol. 29, no. 3, pp. 1481-1489, Jun. 2014.

[7] J. Freytes *et al*., "Improving Small-Signal Stability of an MMC With CCSC by Control of the Internally Stored Energy," in *IEEE Transactions on Power Delivery*, vol. 33, no. 1, pp. 429-439, Feb. 2018,

[8] A. Jamshidifar and D.Jovcic "Small Signal Dynamic DQ Model of Modular Multilevel Converter for System Studies" *IEEE Transactions on Power delivery*, Vol 31, iss 1, February 2016, pp 191-199

[9] A. Gole, V.K. Sood, L. Mootoosamy, "Validation and Analysis of a Grid Control System Using D-Q-Z Transformation for Static compensator Systems" *Canadian Conference on Electrical and Computer Engineering Montreal, PQ, Canada September 17-20 1989, pp 745-748*